Buckling instability of droplet chains in freely suspended smectic films

C. Völtz and R. Stannarius
Otto-von-Guericke-Universität Magdeburg, Institut für Experimentelle Physik, D-39106 Magdeburg, Germany
(Received 23 February 2005; published 15 July 2005)

A buckling instability of chains of isotropic droplets in smectic films is investigated. The *c*-director field in a free-standing film is prepared as a target pattern with a continuous radial deformation. In such a pattern, isotropic liquid droplets are induced by light irradiation of the photochromic mesogenic material. The droplets align tangentially in regular chains in the regular structure of the *c*-director field. Incorporation of additional droplets lengthens the chains at a given ring diameter until they form complete rings. Further chain growth introduces a reversible buckling with a characteristic wave length. The phenomenon is similar in many respects to growth processes in biosystems or Euler buckling in polymer foils. A simple model of the wavelength selection mechanism is introduced.

DOI: 10.1103/PhysRevE.72.011705 PACS number(s): 61.30.−v, 89.75.Fb, 82.70.Kj, 73.50.−h

I. INTRODUCTION

Solids under externally applied stresses and strains exhibit a variety of instabilities. A classical example is the well-known Euler buckling instability of a compressed rod which buckles out sideways if the compression stress exceeds a critical value [1–3].

Such a compression can occur, for example, as a consequence of the growth of the length of a linear structure under lateral geometrical restrictions. Recently, buckling has been reported for free deformed plastic sheets [4]. For such sheets, the bending rigidity is much smaller than the stretching rigidity. Thus, to reduce its elastic energy, the sheet can easily buckle into shapes that remove in-plane compression. It has been suggested, that in leaves a similar increase in length near the edge can result from growth processes, and that the wavy structures in some leaves might be formed in this way.

In a stochastic model, the growth of one-layered tissues (cell chains, respectively) has been studied and folding has been observed [5]. Similar buckling phenomena have been encountered in a simulation of a flexible chain of molecules [6]. It was found that for this system, the wavelength of the buckling grows with increasing time.

Here we report an occurrence of Euler buckling in a very different physical system. It appears in isotropic droplet chains in free-standing smectic films (Fig. 1), structures that are quite similar to chains in electrorheological fluids [7]. In the smectic films, the *c*-director plays the role of the electric field, and the topological defects connected with the droplets are the equivalent of the electric dipoles. We prepare such droplet chains in a regular director structure and control the chain length by influencing the formation of additional droplets with an external parameter in our experiment by illumination of the film with visible light.

In a free-standing smectic film, a director field with a continuous radial deformation in the shape of a spiral or target pattern can be prepared under certain experimental conditions. For that purpose, the coupling of the *c*-director orientation in the anisotropic material (the vector defining the projection of an average mesogenic tilt onto the layer plane) with shear flow or external electric fields is exploited. Target or spiral patterns have been found earlier in vortex flow stimulated, e.g., by mechanical [8–10], thermal [11–13], or electrical [14–20] excitation. In our freely suspended films, with diameters above 1 mm and a submicrometer thickness, the ring pattern forms in the consequence of a thermally driven convective flow in the film plane. The pattern consists of concentric ring-shaped walls formed by the director field around the center of the film. Along the radial coordinate, the orientation of the *c*-director changes continuously, the deformation type alternates from splay to bend (Fig. 2, bottom).

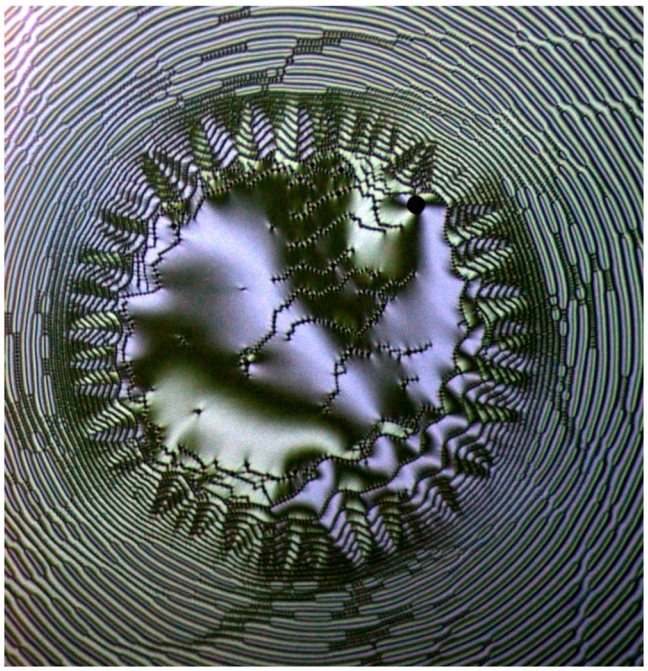

FIG. 1. (Color online) Buckling of isotropic droplet chains in a target pattern of the *c*-director field. The width of the image is 655.2 μm. Individual droplets in the chains are only resolved in the central part of the image; otherwise the chains are recognized by dark lines. The innermost rings are replete and start to develop a modulation pattern with characteristic wavelength. $T=122\,^{\circ}\mathrm{C}$, crossed polarizers. The droplet density decreases toward the outer rings. Details of droplet chains are shown in Figs. 2 and 5.

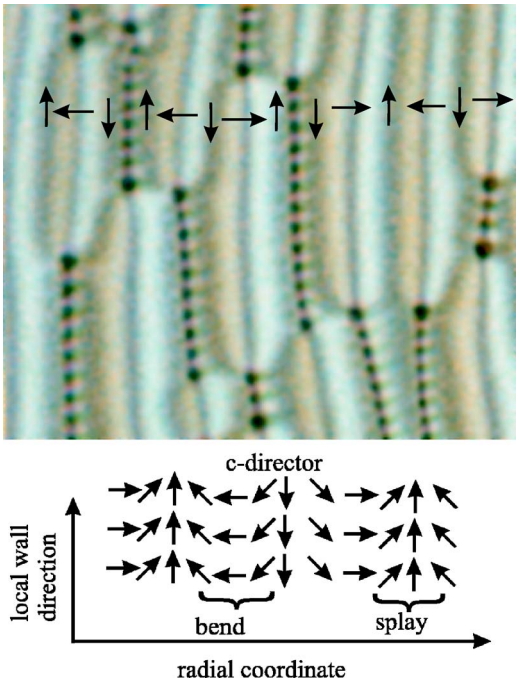

FIG. 2. (Color online) top: reflection image of a target pattern detail with short droplet chains along the local bend regions. The orientation of the *c*-director at selected positions is visualized by arrows. Note that with our observation technique (normal incidence) we cannot distinguish the sense of direction of the arrows, but this is irrelevant for the interpretation of the experiment. Bottom: schematic sketch of the continuously distorted *c*-director orientation.

Isotropic droplets can be created in the film plane by heating the film close to the clearing temperature [21] where locally part of the film material melts into the isotropic liquid state. The droplets in our experiment thus contain the same material as the surrounding smectic film, but in principle one can prepare similar liquid crystal emulsions with other liquids dispersed in the bulk LC phase [22–26]. In the freestanding film geometry, the systems can be considered as quasi two-dimensional emulsions. We exploit the photosensitivity of the azoxy material used in the experiments to control the droplet formation by light illumination as described below. The purpose of this study is the investigation of a reversible buckling process in a system where the length of a chain at a given end-to-end distance (or at a constant circumference of a closed ring, as in our cylindrical geometry) can be controlled by external conditions.

II. EXPERIMENTAL SETUP

The chemical structure of the photochromic material 11OAB (4,4′-bis-*n*-undecyloxy-azoxybenzene) studied here is shown in Fig. 3. The substance has the phase sequence: Cryst. 80.8 °C SmC 121.4 °C isotropic. Under illumination it undergoes a cis-trans isomerization [27]. A growing concentration of cis-isomers leads to a lowering of the order parameter and a decreased clearing temperature.

Films are prepared by drawing a small amount of liquid crystalline material in the SmC state across a hole of radius

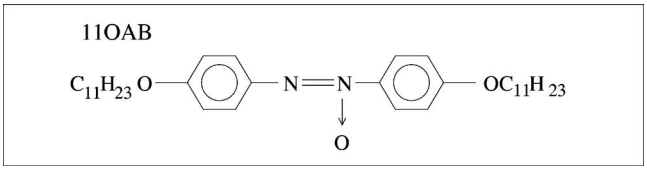

FIG. 3. Chemical structure of the mesogenic material.

ranging between 1 and 3 mm in a support frame.

The support of the film is temperature controlled by a commercial heating stage (Linkam THMS600) with a temperature stability of 0.1 K. However, we note that the intense illumination of the film has a measurable influence on the film temperature, so that the absolute stability of the temperature is estimated to be accurate to ±0.5 K only.

The textures are in general observed between crossed polarizers with an optical microscope (Zeiss Axioskop 40) in reflection mode. In some of the experiments, the polarizers are slightly decrossed in order to distinguish the two diagonal orientations of the *c*-director. Images of the film texture are taken with a charge-coupled device (CCD) camera connected to a computer and processed digitally.

The thickness of all films is in the range between 100 and 200 smectic layers. In the experiments, only films with uniform thicknesses on a molecular level have been evaluated.

III. EXPERIMENTAL RESULTS

In the target pattern of the director field, the dispersed droplets assemble preferentially in chains, in local bend regions of the *c*-director field. The *c*-director field in the vicinity of the droplet chains has been described in detail in Ref. [21], and a comprehensive investigation of the defect structures created by the droplets has been performed there. Figure 4 sketches the *c*-director in the surrounding of droplets. The microscope picture in Fig. 2, top, shows a detail of the structure in a region with few short droplet chains. The image is taken in reflection under (almost completely) crossed polarizers, horizontal and vertical in the image. In the ab-

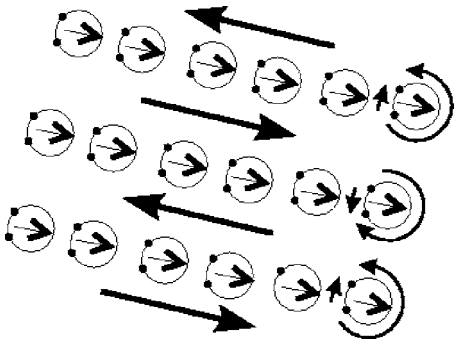

FIG. 4. Sketch of the *c*-director field in the regions filled with droplet chains. Positions of the −1/2 defects on the droplet boundaries are marked with dark bullets. The arrows inside the droplets sketch the direction of the topological dipole associated with the droplet. Neighboring chains do not necessarily have the same directions of these dipoles, but the *c*-director between the chains (straight arrows) alternates in any case.

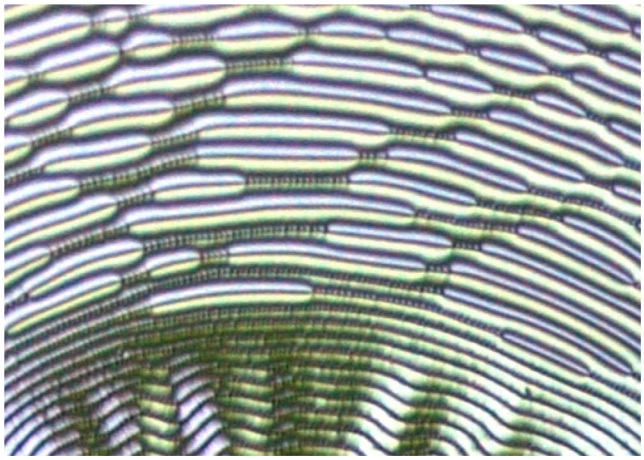

FIG. 5. (Color online) Details of the droplet chain pattern: From top to bottom: Partially filled rings, completely filled smooth rings, and replete rings with buckling. The width of the image is 337.2 μm. Individual droplets are resolved only in the top part of the figure. This may be a hint that the droplet distance in replete rings is compressed somewhat below the equilibrium distance.

sence of droplets, the continuous alternation of bend and splay regions from left to right in the image is reflected by subsequent dark and bright parallel lines. Since the splay elastic constant is larger than the bend constant in the material investigated, the splay regions (c-director in the wall center along the wall) are somewhat broader than undisturbed bend regions (c-director in the wall center perpendicular to the wall), as is seen in the undisturbed top right part of Fig. 2, top. Dark areas indicate regions where the c-director is oriented either along the polarizer or along the analyzer, i.e., horizontally or vertically in the image, along the regions with diagonal director. The different colors in the image (pink and bluish, in the black and white image represented by slightly different grey shades) indicate left and right diagonal c-director orientations. In order to distinguish these orientations by their slightly different colors, the analyzers have been slightly decrossed in this picture. Figure 2 shows that the chains prefer the regions where the c-director points in the direction of the director gradient (bend regions), and the image demonstrates how they contract these regions because of the anchoring conditions at the droplet boundaries. The original c-director structure is seen in the gaps where chains are interrupted (Figs. 2 and 5).

One can also see in the figure that the droplets are monodisperse, except for somewhat larger droplets at the chain ends, and that they have regular spacings in the chains. The chains are aligned exactly tangential in the target pattern. Since the c-director at the droplet surface aligns tangentially, the chains contract the bend regions to a width of the order of the droplet diameter.

With increasing droplet density, the chain segments grow and eventually they combine and form closed circles (see inner rings in Figs. 1 and 5). This gives us the opportunity to investigate the deformation and buckling of droplet chains as a function of chain length, by increasing the number of droplets merging with the chains. Like in biological growth processes, the incorporation of additional material in a closed ring elongates the structure at a given average diameter, such that it becomes unstable and subject to spontaneous buckling. It can be seen in Fig. 1, that the inner rings of the target pattern are first filled up by droplets and start to buckle quite regularly. Two conditions are necessary for the preparation of the initial state of closed-ring chains: a continuous deformation of the director field, with alternating splay and bend domains, and a preferred location of the isotropic droplets chains in the c-director pattern. The necessary precondition for chain buckling is the competition of two forces, a bending rigidity of the chains originating from the interactions of the topological dipoles connected with each droplet, and a limited amplitude of the chain deformations in the director pattern.

It is typical for the material used in our experiment that it builds up periodic stripe patterns in free-standing films in the smectic C phase, even in the absence of shear flow. For the preparation of circular director patterns, we need to initiate a vortex flow in the film that aligns these walls tangentially. Such a shear flow is driven in the films, most likely due to small thermal gradients in the film plane, under sufficient illumination of the sample. We use the microscope lamp to control the illumination. Thereupon the c-director field, i.e., the in-plane orientation of the tilt in the smectic layers, starts to wind up continuously.

The arising regularly structured director field is used to control the formation of droplet chains and to investigate their structure and dynamic behavior. After preparation of a free-standing SmC film, the light illumination intensity is increased. The number of isotropic droplets that emerge in the film increases with temperatures and/or with illumination intensity. Self-organization of the droplets in chain segments starts spontaneously [21]. The droplets form at random positions in the film, i.e., at all orientations of the director field. After their formation, they are forced into existing nearby chains by elastic interactions. The forces involved in this self-organization of chains have been described in detail [21–26,28–31]. Each of the droplets carries two half-integer defects on its boundary. The droplets in the chains are oriented in such a way that the defect pairs point into the same direction. When a long droplet chain is built up from single droplets, the ratio of the equilibrium distance between neighboring droplet centers and the droplet diameters is quite constant. For a different material [21], this ratio has been determined to be 1.28. This value is roughly the same as that obtained for cholesteric droplets in SmC^* films [29,30] where the authors have analyzed chains of a different topology, in which the droplets were separated by isolated $S=-1$ defects in the c-director field. In the mesogenic material 11OAB used here, the droplets are quite small and the ratio of equilibrium droplet distance and droplet diameter cannot be determined with satisfactory accuracy from the microscope images. However, we estimate that it is close to the value given above. For the buckling phenomenon itself, the value of the equilibrium droplet separation is not essential, but the existence of such a well-defined equilibrium separation, which is evidenced by Fig. 2.

In the target patterns, inner rings are filled faster than the outer rings. Figure 5 shows the coexistence of rings with different degrees of filling in the target pattern. From top to

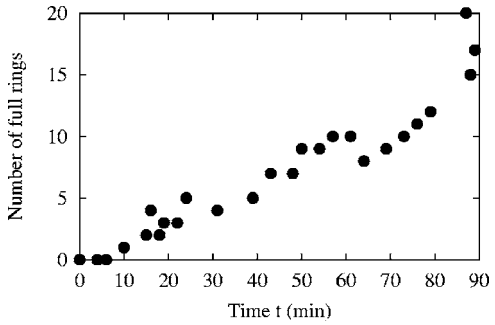

FIG. 6. Number of rings completely filled by droplets as a function of time for a given film of 11OAB, far from saturation. The number of full rings increases with time.

bottom there are partially filled rings, completely filled rings which do not buckle yet, and replete rings which are already undulated with a quite well-defined periodicity and increasing amplitude.

When a circular droplet chain is completely filled by droplets, and more droplets emerge and are incorporated into the chain, then the length of the closed chains increases. This can be considered as an analogy to biological growth processes where each element in a given structure changes its length at a fixed outer contour, by addition of new material. The circumference of the circular rings is fixed, and the rings do not have space to give way, since they are enclosed by the neighboring rings. This leads to the buckling of closed droplet chains. This buckling spreads from the most replete inner rings to the outer rings. The buckling of adjacent rings is strongly correlated, and the amplitude of the undulation grows toward the film center, whereas the average undulation wavelength is preserved. Due to the elastic deformations of the *c*-director field, adjacent chains retain an equilibrium distance even when they are undulated. This is particularly evident in Fig. 5.

With progressing time, more rings are saturated (completely filled) and oversaturated by droplets, and the buckling structure grows from the inner rings to the outside of the target pattern. The observation that under continuous illumination the number of rings completely filled by droplets increases, is demonstrated in Fig. 6. This figure shows the number of completely filled rings as a function of time. The slight variations of the slope of this curve are basically due to small fluctuations in the illumination intensity. Figure 7 shows the temporal evolution of the buckling instability. When the buckling of the chains becomes stronger, the area in the middle of the target pattern is gradually filled with buckled chains, cf. Fig. 7(c). If the illumination intensity is drastically reduced, the droplet density decreases and hence the chains straighten again.

In Fig. 7(c), a Maltese cross is visible in the region of completely filled but undeformed droplet rings. This reflects the orientation of the *c*-director in the surrounding of the droplet chains. As sketched in Fig. 4, the *c*-director in the gap between neighboring chains is parallel to the chains, and in particular it is aligned almost strictly tangential at the boundaries of the individual droplets. The sense of direction is opposite along the two sides of each chain. In the buckled

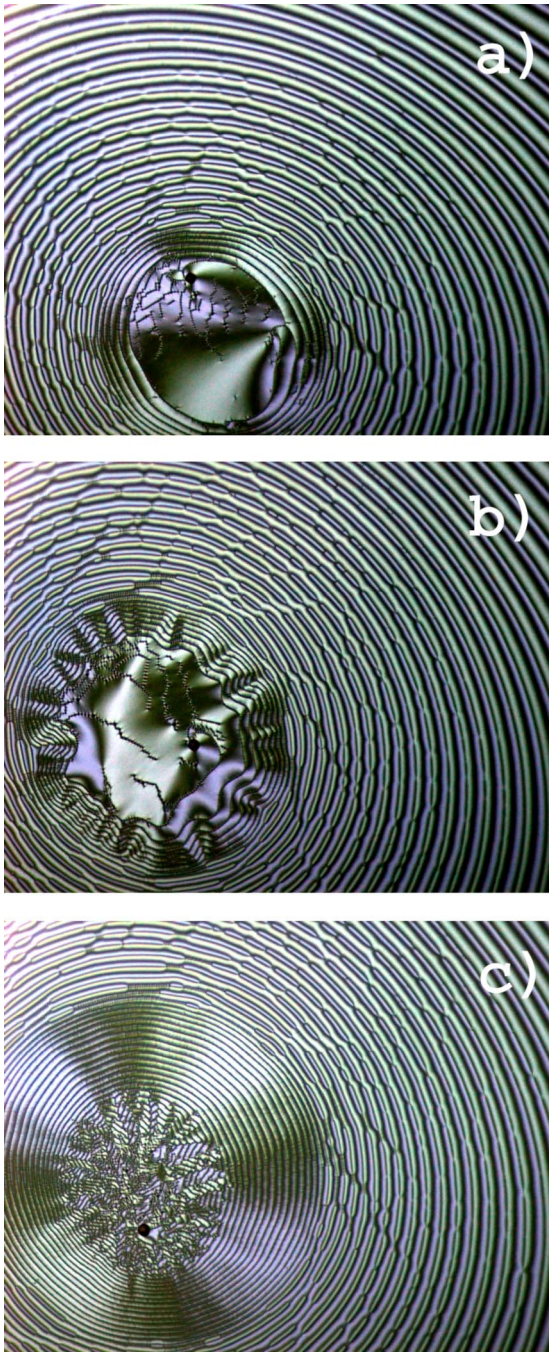

FIG. 7. (Color online) (a) Temporal evolution of the buckling instability of the droplet chains, $T=122\,^{\circ}\mathrm{C}$ for (a) 31 min, (b) 39 min, (c) 85 min after the beginning of illumination, width of the images is 859.6 μm. The inner rings are first filled up by droplets and start buckling with a distinct wavelength. Later, the outer rings are filled up.

regions, the director follows the local chain orientation (Fig. 8), as can be concluded from the optical reflectivity and local chain orientation, e.g., in Figs. 7(b) and 7(c). The buckling driven by the increasing length of the chains has to work against the elastic forces of the director field. Adjacent rings hinder the unlimited growth of the amplitude of chain undulations. The situation is in principle analogous to the Helfrich-Hurault instability in layered materials as, for ex-

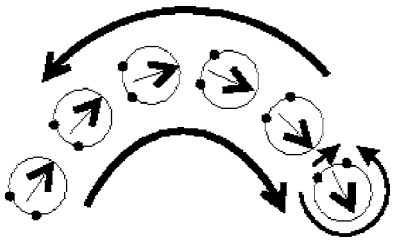

FIG. 8. Sketch of the *c*-director field near a bent chain, see legend of Fig. 4.

ample, smectics under external mechanical or magnetic fields.

The transition from nonbuckling rings to buckling rings shows a critical behavior. This means that a bifurcation to buckling occurs, comparing to the Euler buckling of a rod. This bifurcational behavior is shown in Figs. 9(a)–9(c), where the degree of filling is shown as a function of ring number, counted from the innermost ring in the target pattern. A filling of 100% means that the rings are completely filled by droplets. In Fig. 9(a) some of the inner rings of the target pattern are completely filled by droplets, but no buckling occurs yet. In Figs. 9(b) and 9(c) buckling occurs. Left of the vertical line the buckling of the rings occurs, and right of the vertical line, no buckling occurs. The wavelength of the undulation is constant in time, and the buckling is reversible: As soon as the light illumination intensity is decreased, the number of droplets decreases as well, and the undulation amplitude decays.

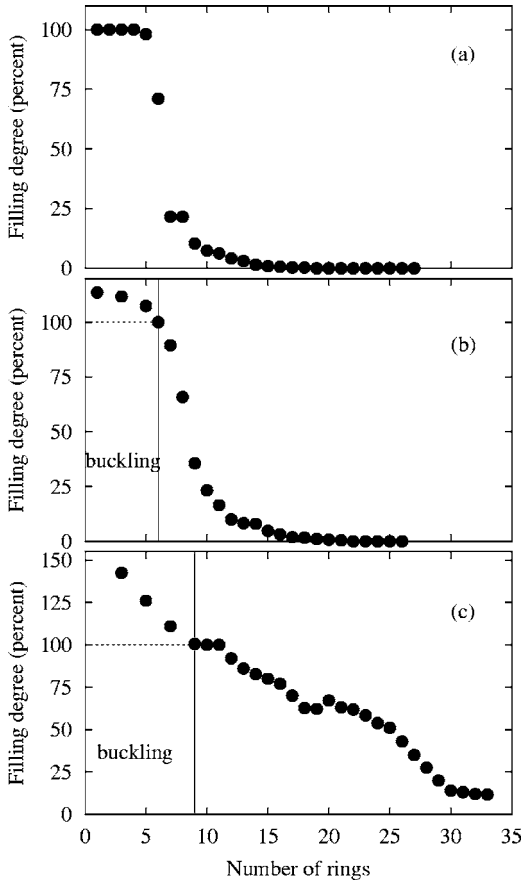

FIG. 9. Degree of filling of droplet chains for (a) 31 min, (b) 39 min, and (c) 76 min after start of illumination. The rings on the right of the vertical line are incompletely filled; they contain short, isolated chain segments. The rings on the left of the vertical line show buckling. The data give the ratio of the chain length to the length of a circular chain at the same average position.

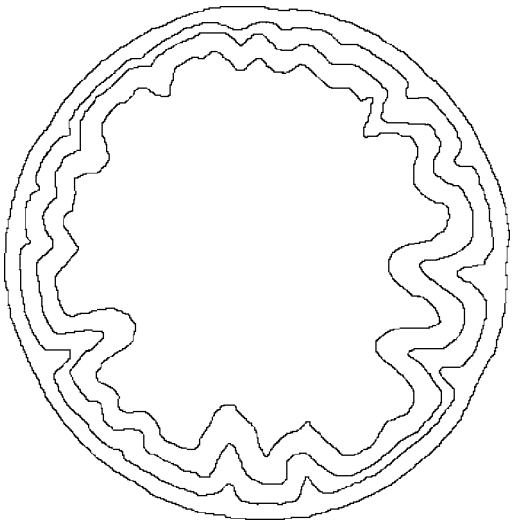

FIG. 10. Buckling of droplet chains at $t=76$ min. Four digitally extracted chains are marked and analyzed. The width of the image is 376.8 μm.

For further quantitative analysis, droplet rings are digitally extracted from the images. This is demonstrated exemplarily with four chains in Fig. 10. The positions of the lines are extracted and "stretched out," i.e., the distance from the target center is plotted versus the angular coordinate. Then, they are digitally processed. The lengths of the lines are calculated and the ratio of this length and the length of the circumference of a circle with the same mean radius is calculated. For the outer chain in Fig. 10, this ratio is about one. Due to the increase in the undulation amplitude, this number increases toward the center of the pattern. It is 1.1 for the second ring, 1.3 for the third ring, and 1.4 for the innermost ring. In Fig. 9, the filling of the outer rings and the length of buckled inner chains are composed in one plot. In the first diagram (a), the inner rings are completely filled with droplets, but the oversaturation of the central rings can be compensated by a compression of the chains, i.e., the decrease of the equilibrium distance between adjacent droplets in the chain. In the following picture (b), the instability has set in, the compression of the chains is relieved, and has been replaced by an undulation of the chain. The trend of the filling of outer rings, i.e., droplets density per length, is continued in the length to circumference ratio. Due to the high sensitivity to small temperature and illumination parameters, the structures are dynamic, as is seen in Fig. 6, the rings are not filled monotonically, but with slight fluctuations. Therefore, the number of completely filled but not undulated rings varies. In general, there is a small zone of such rings, this is indicated in the final picture (c), and most pronounced in Fig. 7(c). In these rings, we assume that the chains are under lateral strain.

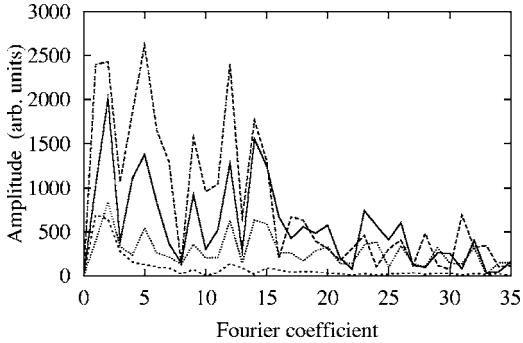

FIG. 11. Spectra of the four lines in Fig. 10 at $t=76$ min. The Fourier coefficients are normalized in periods per full circle. All buckled lines show contributions of essentially the same Fourier coefficients, between 2 and 15. The dashed line represents the spectrum of the outermost ring in Fig. 10, the solid line the second ring from inside, the small dotted line the third ring, and the big dotted line the outermost ring.

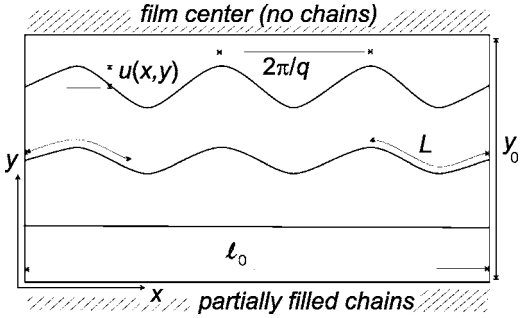

FIG. 12. Model geometry of the chain deformation and wavelength selection (see text).

Quantitative information on the undulation wavelengths can be obtained from Fourier spectra of the undulated lines. We have calculated Fourier spectra for four representative lines shown in Fig. 10. The lines have been "unrolled" as described above, i.e., the distance from the center is plotted as a function of the angular coordinate. Then, the Fourier transformation has been performed and the absolute peak intensities have been compared in Fig. 11. The coefficients have been normalized such that the first coefficient yields the contribution of one deformation period per full circumference. The 0th coefficient, which is set to zero, gives the radius of the undeformed ring. Coefficient 1 is related to the correct choice of the center of the pattern. It can be neglected, since it corresponds only to an offset of the center of the circle. The essential contributions to the spectra are found between coefficients 2 and 15. The spectra of all three undulated rings show essentially the same shape of the Fourier spectrum, i.e., the undulations have wavelengths with 2 to 15 periods per circumference. The dominant Fourier coefficients do not significantly change in time (data not shown).

IV. MODEL AND DISCUSSION

The increasing length of droplet chains with a constant circumference induced by light illumination leads to the buckling instability, which has many similarities with the above-mentioned buckling of plastic sheets [4] or the buckling of growing organisms like the petals of the petunia. When the edge of the petal grows in length, this leads to the wrinkling of the petal.

In order to understand the possible principle mechanism for the pattern selection, it may be useful to consider a related phenomenon in smectic A liquid crystalline samples under the influence of a force that stretches the sample normal to the layers. The Helfrich-Hurault (HH) instability leads to the buckling of smectic layers that compensates the dilatation pressure. A characteristic wavelength is selected there which depends upon the ratio of the elastic constants for curvature elasticity and smectic layer compression, and upon the dimension of the sample. A direct transfer of the analytical expressions for the wavelength selection to our system is not possible. However, we will assume that two mechanisms control the buckling period: First, there is a force that keeps the chains of droplets straight. This force is equivalent to the curvature elasticity term in the HH situation. Second, we assume that there is some equilibrium distance between adjacent undeformed droplet chains. We conclude that from the fact that the center of the film is almost chain free whereas the rings around this central "tornado eye" appear to have a rather well-defined separation, see in particular Figs. 1 and 7(a). This provides some equivalent to the smectic layer spacing.

The droplet chains will consequently be considered as the equivalent of the smectic layer structure in this model, and we treat the problem in a Cartesian geometry, i.e., instead of considering circular chains in a target pattern, we assume in first approximation a rectangular area where chains extend from the left to the right edge (Fig. 12), the width ℓ_0 be equivalent to the length of a completely filled droplet chain (filling factor 1.0). The coordinates are x in the direction of the undeflected chains, y perpendicular to it. This model is appropriate when one describes the undulation of droplet chain arrays in a sufficient distance from the film center.

When we discuss energies that are connected with the chain arrangements, we will express them in terms of free energy densities. As all interactions are mediated via the smectic film, the forces between droplets and chains depend linearly upon the film thickness. Since all forces considered here have the same linear film thickness dependence, it is sufficient to discuss the specific energies per volume.

Energies that are relevant for the problem are the compression energy W_L of the chains, i.e., the energy that is necessary to reduce or increase the droplet-droplet distance in a straight chain. The second energy contribution W_K is related to the curvature of the chains and of the related bend of the director field in the gap between the chains. This term can be considered as an effective bending rigidity of the chains, and treated analogous to the curvature elasticity in the HH problem.

$$W_K = \frac{1}{2} K u_{xx}^2.$$

We note that the force constant K is not simply equal to any of the curvature elastic constants of the smectic material,

although a direct relation between the orientational elasticity and the chain flexibility must exist. The third energy term W_B describes the interchain potential.

$$W_B = \frac{1}{2} B u_y^2.$$

This presupposes some equilibrium droplet chain distance. While at the present stage, we have no theoretical foundation for the existence of such a preferred chain-chain distance, experimental evidence supports this assumption, see discussion above.

We assume a sinusoidal deformation $u(x,y) = \tilde{u}(y)\cos(qx)$, where $\tilde{u}(y)$ is the amplitude of the undulation of a given chain, a simple y dependence can be described by $\tilde{u}(y) = u_0 \sin(q_y y)$, with a quarter sinus period in the box, $q_y = \pi/2y_0$. The length of an undulated chain

$$\ell = \int_0^{\ell_0} \sqrt{1 + u'^2}\,\mathrm{d}x \approx (1 + \tilde{u}^2 q^2/4)\ell_0$$

depends upon undulation wave-number q and amplitude $\tilde{u}(y)$. In agreement with experimental observations, we assume that the droplet density in the rings increases toward the film center. The local supersaturation Δ (ratio of excess droplet density and droplet density in the completely filled straight chain) is given by the ratio of the length $L = [1 + \Delta(y)]\ell_0$ of an uncompressed chain that contains all droplets at position y and the container dimension ℓ_0. If one allows for chain compressibility, the energy necessary to compress such a chain may be described by the ansatz (Hooke's law)

$$W_L = \frac{\gamma}{2\ell_0}(\ell - L)^2,$$

with the force constant γ. We will assume here that the chain is practically incompressible, i.e., γ is very large, and $\ell = L$. Then, the relation $\Delta(y) = 1/4\tilde{u}(y)^2 q^2$ is strictly fulfilled, which relates the amplitude $\tilde{u}(y)$ to the wave number q. In particular, when the maximum supersaturation is denoted by $\Delta_{\max} = \Delta(y_0)$, we can set

$$u_0 = 2\sqrt{\Delta_{\max}}/q.$$

In that case, we can insert these relations into the equations

$$W_K = \frac{1}{2} K u_0^2 \sin^2(q_y y)\cos^2(qx) q^4,$$

$$W_B = \frac{1}{2} B u_0^2 \cos^2(q_y y)\cos^2(qx),$$

and exclude W_L in the following energy evaluation.

We average the total energy $W = W_K + W_B$ over the pattern, with $\overline{\cos^2(qx)} = \overline{\cos^2(q_y y)} = \overline{\sin^2(q_y y)} = 1/2$.

$$\bar{W} = \frac{1}{8} K q^4 u_0^2 + \frac{1}{8} B q_y^2 u_0^2 = \frac{\Delta_{\max}}{2}(K q^2 + B q_y^2 q^{-2}).$$

The minimum deformation energy is found for an undulation with wave-number

$$q_C = \left(\frac{\pi^2}{4y_0^2}\frac{B}{K}\right)^{1/4}.$$

While this simple model does not provide a quantitative description of the undulation, in particular since we have no information about the relative magnitudes of the involved parameters B and K, it yields a qualitative understanding of the wavelength selection mechanism. However, there is a realistic chance to relate these quantities to the elastic constants of the smectic material if a rigorous calculation of the director fields is achieved, since we do not assume other than curvature elastic forces between the droplets in a uniformly thick film area.

When one assumes a certain compressibility of the chains (corresponding to the choice of a lower γ), then one may even find a critical compression or supersaturation for the onset of buckling, since W_L grows with the square of $\Delta_{\max}$ while the distortion energies increase only linearly in $\Delta_{\max}$. In that case, an excess of droplets will first be compensated by a slight compression of the intrachain droplet distances before buckling sets in. This is actually indicated in the experimental data (Fig. 9). A detailed analysis is found in [32].

V. SUMMARY

The buckling of droplet chains in smectic C free-standing films has been investigated. When the c-director field in the film is prepared as a target pattern with a continuous radial deformation and micrometer droplets are produced in the film plane, a preferred location of the droplets is found in the bend-regions of the c-director field. The droplets self-organize in rings of bend director orientation. Once rings are completely filled, the chains are saturated. The formation of additional droplets (supersaturation) lengthens these chains, introducing a reversible buckling with a characteristic wavelength. The buckling of adjacent rings is in phase, and the main wavelength does not significantly change in time. A qualitative model for the wave length selection mechanism is presented. The perspectives of the system to describe buckling phenomena as they are common in many other physical and biological systems lies in particular in the reversibility of the structure formation. When the number of droplets is controlled, e.g. by temperature or light variation, the supersaturation can be reversibly influenced and the effects on the reorganization of the chain structures can be studied experimentally. There is a good chance to get quantitative access to the involved model parameters when the director field around the chains and the related elastic energies are calculated numerically and a relation to the well known curvature elastic constants is established.

ACKNOWLEDGMENTS

The authors cordially thank Wolfgang Weissflog for the supply of the mesogenic material, A. Eremin, Ch. Bohley, and G. Pelzl are acknowledged for fruitful discussions. This study has been partially supported by DFG Grant No. STA 425/17.

[1] L. D. Landau and E. M. Lifshitz, *Theory of Elasticity* (Pergamon, New York, 1986); A. E. Love, *A Treatise on the Mathematical Theory of Elasticity* (Dover, New York, 1944).
[2] J. P. Den Hartog, *Strength of Materials* (Dover, New York, 1977).
[3] L. Golubovic, D. Moldovan, and A. Peredera, Phys. Rev. E **61**, 1703 (2000).
[4] E. Sharon, B. Roman, M. Marder, G.-S. Shin, and H. L. Swinney, Nature (London) **419**, 579 (2002).
[5] D. Drasdo, Phys. Rev. Lett. **84**, 4244 (2000).
[6] L. Golubovic, D. Moldovan, and A. Peredera, Phys. Rev. Lett. **81**, 3387 (1998).
[7] W. M. Winslow, U.S. Patent No. 2,417,850 (25 March 1947); J. Appl. Phys. **20**, 1137 (1949); H. Block, J. P. Kelly, A. Qin, and T. Watson, Langmuir **6**, 6 (1990).
[8] P. E. Cladis, Y. Couder, and H. R. Brand, Phys. Rev. Lett. **55**, 2945 (1985).
[9] I. Mutabazi *et al.*, Europhys. Lett. **19**, 391 (1992).
[10] D. Dash and X. L. Wu, Phys. Rev. Lett. **79**, 1483 (1997).
[11] Y. Marinov and P. Simova, Liq. Cryst. **12**, 657 (1992).
[12] M. I. Godfrey and D. H. Van Winkle, Phys. Rev. E **54**, 3752 (1996).
[13] J. Birnstock and R. Stannarius, Mol. Cryst. Liq. Cryst. Sci. Technol., Sect. A **366**, 815 (2001); R. Stannarius and J. Birnstock, Phys. Rev. Lett. **86**, 4187 (2001).
[14] G. Hauck and H. D. Koswig, Ferroelectrics **122**, 253 (1991).
[15] P. E. Cladis, P. L. Finn, and H. R. Brand, Phys. Rev. Lett. **75**, 1518 (1995).
[16] J. Maclennan, Europhys. Lett. **13**, 435 (1990).
[17] R. Stannarius, C. Langer, and W. Weißflog, Phys. Rev. E **66**, 031709 (2002).
[18] A. Becker, H. Stegemeyer, R. Stannarius, and St. Ried, Europhys. Lett. **39**, 257 (1997).
[19] C. Langer and R. Stannarius, Phys. Rev. E **58**, 650 (1998).
[20] D. Link *et al.*, Phys. Rev. Lett. **84**, 5772 (2000).
[21] C. Völtz and R. Stannarius, Phys. Rev. E **70**, 061702 (2004).
[22] H. Stark, Phys. Rep. **351**, 387 (2001) and references therein.
[23] P. S. Drzaic, *Liquid crystal dispersions* (World Scientific, Singapore, 1995), Vol. 1.
[24] P. Poulin, H. Stark, T. C. Lubensky, and D. A. Weitz, Science **275**, 1770 (1997).
[25] P. Poulin, V. Cabuil, and D. A. Weitz, Phys. Rev. Lett. **79**, 4862 (1997).
[26] P. Poulin and D. A. Weitz, Phys. Rev. E **57**, 626 (1998).
[27] Ch. Leier and G. Pelzl, J. Prakt. Chem. **321**, 197 (1979).
[28] V. K. Dolganov, E. I. Demikhov, I. Fouret, and C. Gors, Phys. Lett. B **220**, 242 (1996).
[29] P. Cluzeau, P. Poulin, G. Joly, and H. T. Nguyen, Phys. Rev. E **63**, 031702 (2001).
[30] P. Cluzeau, V. Bonnand, G. Joly, V. Dolganov, and H. T. Nguyen, Eur. Phys. J. E **10**, 231 (2003).
[31] P. V. Dolganov, E. I. Demikhov, V. K. Dolganov, B. M. Bolotin, and K. Krohn, Eur. Phys. J. E **12**, 593 (2003).
[32] R. Stannarius and C. Völtz, Phys. Rev. E (to be published).